

# Tissue Deformation Modulates Twist Expression to Determine Anterior Midgut Differentiation in *Drosophila* Embryos

Nicolas Desprat,<sup>1</sup> Willy Supatto,<sup>1,2</sup> Philippe-Alexandre Pouille,<sup>1</sup> Emmanuel Beaurepaire,<sup>2</sup> and Emmanuel Farge<sup>1,\*</sup>

<sup>1</sup>Mechanics and Genetics of Embryonic and Tumoral Development Group, UMR168 CNRS, Institut Curie, 11 rue Pierre et Marie Curie, F-75005, Paris, France

<sup>2</sup>Laboratory for Optics and Biosciences, Ecole Polytechnique, CNRS and INSERM U 696, 91128 Palaiseau, France

\*Correspondence: [efarge@curie.fr](mailto:efarge@curie.fr)

DOI 10.1016/j.devcel.2008.07.009

## SUMMARY

Mechanical deformations associated with embryonic morphogenetic movements have been suggested to actively participate in the signaling cascades regulating developmental gene expression. Here we develop an appropriate experimental approach to ascertain the existence and the physiological relevance of this phenomenon. By combining the use of magnetic tweezers with *in vivo* laser ablation, we locally control physiologically relevant deformations in wild-type *Drosophila* embryonic tissues. We demonstrate that the deformations caused by germ band extension upregulate Twist expression in the stomodeal primordium. We find that stomodeal compression triggers Src42A-dependent nuclear translocation of Armadillo/ $\beta$ -catenin, which is required for Twist mechanical induction in the stomodeum. Finally, stomodeal-specific RNAi-mediated silencing of Twist during compression impairs the differentiation of midgut cells, resulting in larval lethality. These experiments show that mechanically induced Twist upregulation in stomodeal cells is necessary for subsequent midgut differentiation.

## INTRODUCTION

The development of a multicellular organism requires that the cells divide, differentiate, and move relative to each other. Precise patterning of gene expression determines the regions in the embryo that undergo active morphogenetic movements such as invagination, extension, or migration (Costa et al., 1993; Keller, 2002; Solnica-Krezel, 2005). Conversely, it has not yet been demonstrated whether endogenous mechanical deformations do also modulate gene expression. In the *Drosophila* ovary, border cells were found to accumulate the transcriptional factor MAL-D (a determinant involved in cytoskeletal dynamics) in their nucleus in correlation to stretching by their migrating neighbors during oogenesis (Somogyi and Rorth, 2004). In addition, numerical simulations suggested that mechanical pressure could regulate cell division rate in wing imaginal discs (Hufnagel et al., 2007). Finally, the expression of some of the earliest embry-

onic patterning genes, such as *twist* in stomodeal cells, was shown to be modulated by artificial deformations at the onset of gastrulation (Farge, 2003). However no direct experiment has shown that Twist upregulation in the stomodeum stems from the endogenous compression generated by gastrulation movements in wild-type embryos. Indeed, the demonstration of functional mechanical induction during development was hampered by the lack of experimental tools controlling the deformation state of specific cells in a living embryo under physiologically relevant conditions. Moreover, the implications of such mechanosensitive gene expression in subsequent embryonic development remained entirely unknown.

Here we investigate *in vivo* the mechanical induction of Twist in stomodeal cells, using controlled forces to produce a deformation comparable to the physiological deformation experienced by stomodeal cells due to germ band extension (GBE) at the onset of gastrulation. For that purpose, we designed a tissue micro-manipulation assay based on magnetic tweezers and magnetic nanoparticle microinjection. This allowed us to control the force exerted on stomodeal cells by its neighboring tissue to mimic the symmetry and the dynamics of the endogenous deformation generated by GBE. We applied this procedure under conditions in which GBE-dependent stomodeal cells' compression was previously prevented by femtosecond pulse-induced ablations (Supatto et al., 2005). We then analyzed the consequences of that operation on Armadillo/ $\beta$ -catenin (Arm) activation and subsequent Twist expression. We also assayed the involvement of Src, a kinase known to regulate junctional E-cadherin-associated Arm (Takahashi et al., 2005), in this mechanotransduction pathway inducing Twist expression. Finally, we explored the downstream physiological function of this mechanical induction: RNAi-based assays were used to downregulate specifically Twist expression in the stomodeum during compression to the basal level measured in the absence of compression. This enabled us to investigate the incidence of Twist expression level on the downstream differentiation of the derivative anterior midgut cells.

## RESULTS

### Regulation of Twist Expression by Tissue Deformation in Stomodeal Cells

In wild-type embryos, the expression of Twist increases in correlation with the compression of stomodeal cells by germ-band

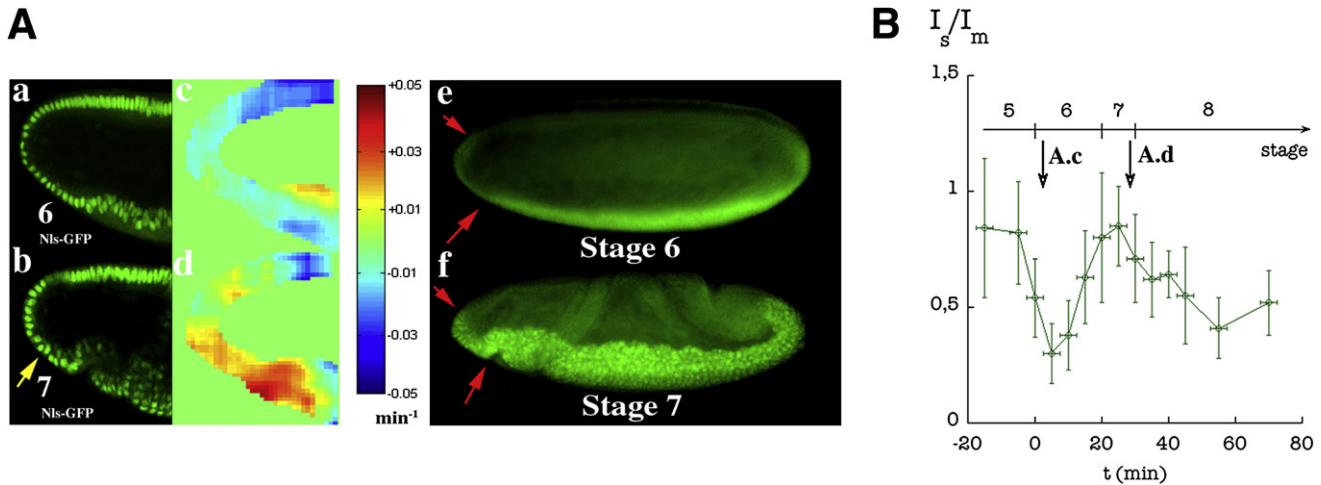


**Figure 1. Dynamics of Twist Expression in Stomodeal Cells at Early Gastrulation**

(A) Mean sagittal deformation rates estimated from nuclear position (Nls-GFP in [a and b]) and velocimetric analysis (c and d) at the beginning of stage 6 ([a and c] before GBE) and mid-stage 6 ([b and d] initiation of GBE). Yellow arrow denotes perturbed organization of nuclei that is characteristic of the initiation of stomodeum compression at this stage. In the compression analysis (see [Experimental Procedures](#)), red is compression and blue is dilation. (e) Low Twist expression in uncompressed stomodeal cells (between red arrows) at the onset of gastrulation (early stage 6). (f) High stomodeal Twist expression after compression initiated by GBE from 20–30 min after the onset of mesoderm invagination (late stage 7).

(B) Twist expression profile: the ratio of stomodeal-to-mesodermal expression ( $I_s/I_m$ ) as a function of developmental stage in wild-type embryos. Time zero corresponds to the onset of gastrulation at the initiation of mesoderm invagination. Each point represents 10 samples. Error bars are standard deviations. Notations A,c and A,d refer to Figure 1A.

extension (Figure 1A control). We measured the ratio of stomodeal-to-mesodermal Twist expression  $I_s/I_m$  to be  $30\% \pm 13\%$  ( $n = 10$ ) at the onset of gastrulation (early stage 6), and to reach a mean value of  $71\% \pm 19\%$  ( $n = 23$ ) after the initiation of GBE (from stage 7 to earliest stage 8; Figure 1B).

To test whether Twist is mechanically induced in stomodeal cells in response to the endogenous compression strains, we first locally ablated the cells responsible for exerting force on the stomodeal primordium, and then used two independent micromanipulation approaches to restore deformations. We used intravital femtosecond pulse-induced ablation to disrupt the most dorsal cells of a wild-type embryo (Figure 2Aa). Subsequent alterations of cell movements corresponding to the first rapid phase of GBE (Irvine and Wieschaus, 1994) prevented the compression of stomodeal cells (Figures 2Ab and 2Ac). Concomitantly, Twist expression markedly dropped in these cells ( $I_s/I_m = 18\% \pm 10\%$ ,  $n = 49$ ) at stage 7 (Figures 2Ad and 2D). In this article, we refer to embryos treated in this manner as “ablated.” Next, we deformed anterior pole cells using a micromanipulated needle. We refer to these embryos as “ablated indented.” A similar approach had previously proven to be successful within the context of a *bcd*, *nos*, *tsl* GBE-defective mutant, in which stomodeal cells were not fully differentiated due to maternal mutations in *torso-like* and *bicoid* genes (Farge, 2003). Here we examined Twist mechanical induction in fully differentiated wild-type stomodeal cells in response to an external deformation. The  $50\ \mu\text{m}$  tip indented the stomodeum by a  $20\ \mu\text{m}$  depth for 10 min during mid-stage 6, corresponding to the time scale of the endogenous onset of compression due to GBE (Figure 2Ba). This external mechanical stress deforms stomodeal cells along a direction perpendicular to their apico-basal axis, except at the tip of the embryo (Figure 2Bb). Embryos were fixed 10 min after the manipulation. In

these embryos, we measured a  $I_s/I_m$  ratio of  $70\% \pm 23\%$  ( $n = 36$ ), i.e. on the order of magnitude of the level of expression of Twist in the control at stage 7 (Figure 2Bd and 2D).

Then, we tested in compression-defective ablated embryos whether an imposed deformation rate similar to the endogenous tissue deformation of intact embryos could rescue stomodeal Twist expression. We designed a micromanipulation assay based on ferrofluid injection into the antero-dorsal cells of the living embryo. This enabled us to manipulate the magnetized cells with magnetic tweezers. First we ablated the dorsal cells of stage 5 embryos, to block endogenous compression forces arising from GBE; then, before cellularization was complete, we injected ferrofluid (magnetic nanoparticles) into the yolk next to the cellularization front. We concentrated the ferrofluid into a patch of roughly 50 anterodorsal cells surrounding the presumptive stomodeum primordium (Figure 2Ca) using an electromagnet. We refer to these embryos as “ablated injected.” Finally, after cellularization completed, magnetic tweezers were used to drag magnetized tissue toward the stomodeum at mid-stage 6 for 10 min. By adjusting the distance between the tweezers and the embryo, we controlled the compression state of stomodeal cells via the force applied to magnetized cells. We could therefore induce tissue deformation mimicking GBE-triggered endogenous deformation. We rescued the mean endogenous sagittal compression rate of stomodeal cells tissue of  $\sim 2\% \text{ min}^{-1}$ , by applying a magnetic gradient of  $120\ \text{T m}^{-1}$  generating a force of  $60 \pm 20\ \text{nN}$  on the stomodeum of the ablated embryos (Figures 2Cb and 2Cc; see Figure S1 and Movie S1 available online). We refer to these embryos as “ablated rescued.” We verified that the photoablation and injection procedures did not induce nonspecific perturbations on dorso-ventral axis signaling by examining the expression of Sim in the neuroectoderm at stage 8, the

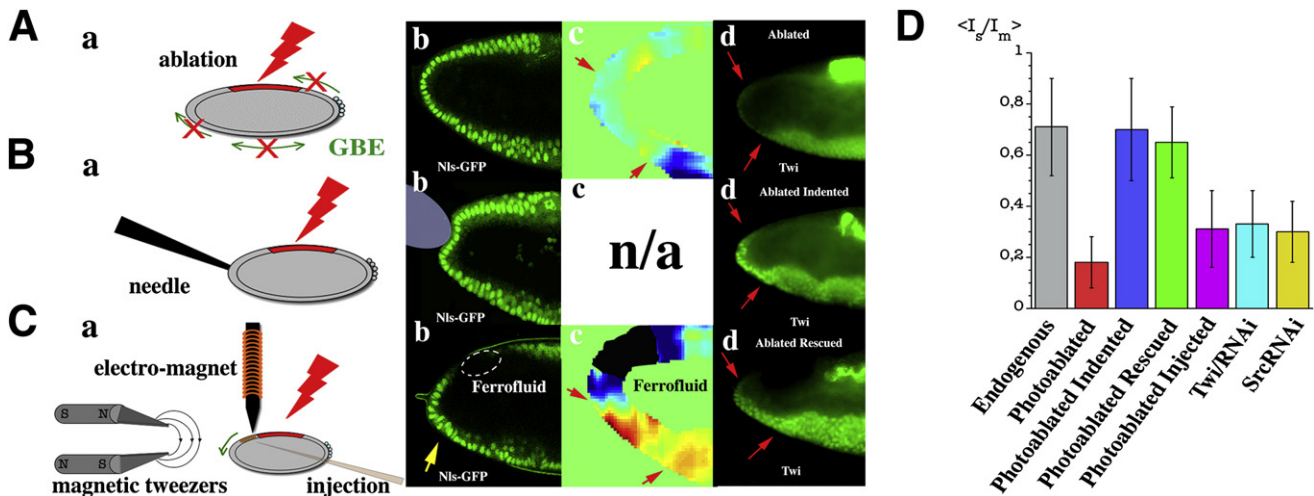


**Figure 2. Mechanical Compression Controls Twist Expression**

(A–C) Photoablation (red in [a]) is used in all experiments shown, to prevent GBE-related movements that normally induce stomodeum compression (green denotes the direction of force propagation in [Aa and Ca]). In each panel, the anterior end of a stage 7 embryo is shown. Nls-GFP (b) is used to visualize nuclei, PIV analysis (c) shows spatial distribution of compression forces (blue pattern at the anterior pole in [Cc] reflects out-of-focus cell movements), and Twist immunofluorescence (d) is shown in green. Yellow arrow denotes disturbed organization of nuclei characteristic of stomodeum compression. (D) Quantitative comparison of Twist expression levels in late stage 7 stomodeal cells. Error bars are standard deviations.

transcription of which is initiated at early stage 6 subsequent to experimental manipulations (Figure S2). We additionally checked normal embryonic morphogenesis after injection until the end of stage 8 (Figure S3 and Movie S2).

The  $I_s/I_m$  Twist expression ratio was  $65\% \pm 14\%$  ( $n = 25$ ) after magnetic compression rescue, compared to  $31\% \pm 13\%$  ( $n = 24$ ) for ablated-and-injected embryos without compression rescue (Figures 2Cd and 2D). The level of Twist expression after magnetic rescue in photoablated embryos is consistent with that seen in control embryos at stage 7 (Figure 2D). Thus, rescuing the compression of the stomodeum, with deformation rate similar to the endogenous dynamics and symmetry of deformation generated by the GBE morphogenetic movement, restores the high level of Twist expression normally observed at stage 7. These experiments demonstrate that during normal development Twist is mechanically upregulated in stomodeal cells at stage 7 by the endogenous morphogenetic movement of GBE.

### Tissue Deformations Activate Armadillo Nuclear Translocation in Wild-Type Embryos

Mechanical signaling has been suggested to be mediated through many pathways, including the activation of cell-cell adhesion complexes (Chen et al., 2004; Matthews et al., 2006). Mechanically-induced nuclear translocation of Armadillo/ $\beta$ -catenin (Arm) has been proposed to control the expression of Twist in stomodeal cells at stage 7 (Farge, 2003). Arm is a major component of cell-cell junctions linked to E-cadherins, and acts as a coactivator for TCF when translocated into the nucleus (Heasman et al., 1994; Nelson and Nusse, 2004; Sanson et al., 1996). Interestingly, mechanically induced nuclear translocation of  $\beta$ -catenin was also observed in mouse bone embryonic development (Hens et al., 2005; Norvell et al., 2004).

Nuclear translocation of Armadillo in *Drosophila* stomodeal cells is observed at the onset of GBE (stage 7), and is lost in ab-

lated embryos (Figure 3A, stage 7 photoablated control). We found using immunofluorescence labeling that this translocation is rescued by both the needle indentation and the magnetic compression assays (Figure 3A photoablated indented and photoablated rescued). DAPI was systematically used as a counterstain to check that confocal images crossed stomodeal cell nuclei (data not shown). We also used immunofluorescence (see Experimental Procedures) to quantify the total level of Arm protein and its preferential allocation to the nucleus (N/J) or cytoplasm (C/J), as compared to junctional regions of the cell. Compared to late stage 5-early stage 6, the ratios were enhanced by a factor of  $\alpha_{N/J} = 2.44 \pm 0.5$  and  $\alpha_{C/J} = 1.55 \pm 0.25$ , respectively ( $n = 15$ ), at stage 7 after endogenous compression by GBE (Figure 3B for  $\alpha_{N/J}$ ). In the case of photoablated embryos, a statistically significant decrease of these ratios to fluctuation levels was found between stage 5 and 7 ( $\alpha_{N/J} = 1.34 \pm 0.36$  and  $\alpha_{C/J} = 1.18 \pm 0.34$ ,  $n = 19$ ) (Figure 3B for  $\alpha_{N/J}$ ) compared to the control ( $p < 0.001$  by Student's t test). Remarkably, the increase was rescued when stomodeal cells were indented with a needle ( $\alpha_{N/J} = 2.05 \pm 0.5$  and  $\alpha_{C/J} = 1.62 \pm 0.38$ ,  $n = 28$ ) or when their compression was rescued with magnetic compression ( $\alpha_{N/J} = 2.25 \pm 0.5$  and  $\alpha_{C/J} = 2.06 \pm 0.4$ ,  $n = 13$ ) (Figure 3B for  $\alpha_{N/J}$ ). We did not observe significant changes in total Arm levels during the course of these experiments (see Supplemental Results). Thus, consistent with Twist expression, the nuclear localization of Arm is mechanically induced in response to the stomodeal compression exerted by native morphogenetic movements.

To assess whether the observed nuclear concentrations of Arm are likely sufficient to exert significant transcriptional effects, we compared the nuclear accumulation of Arm in stage 7 compressed stomodeal cells, with transcriptionally active Arm in Wingless/Wnt-responding cells at stage 9 (Peifer and Wieschaus, 1990). Comparing uncompressed stage 5-stage 6 cells with compressed stage 7 cells, we found that the relative fraction of

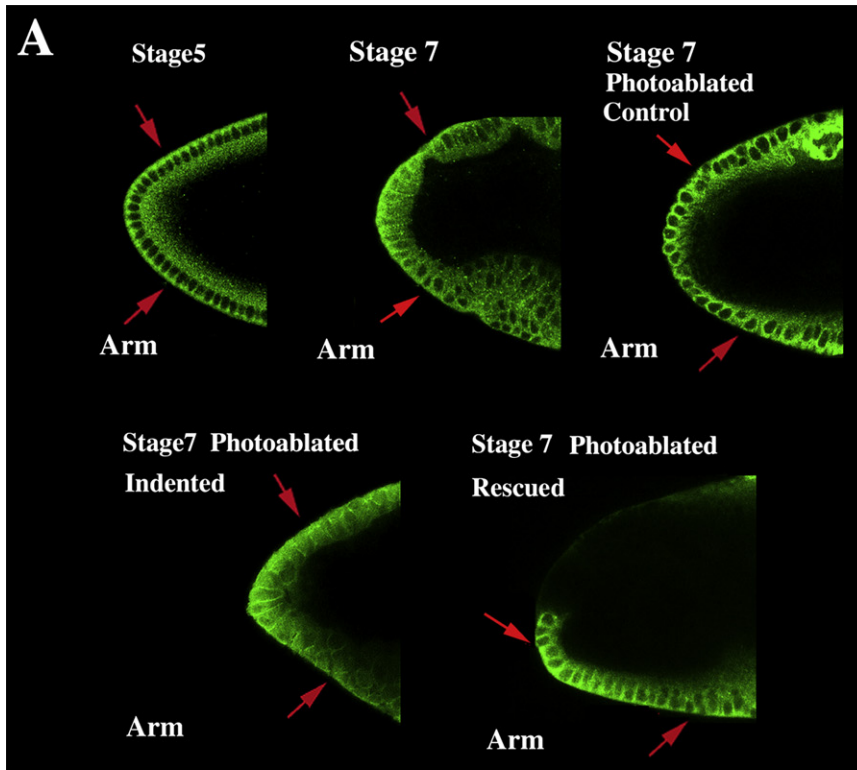
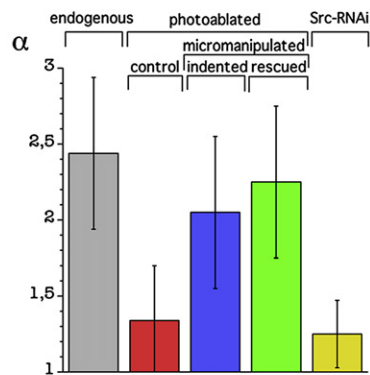


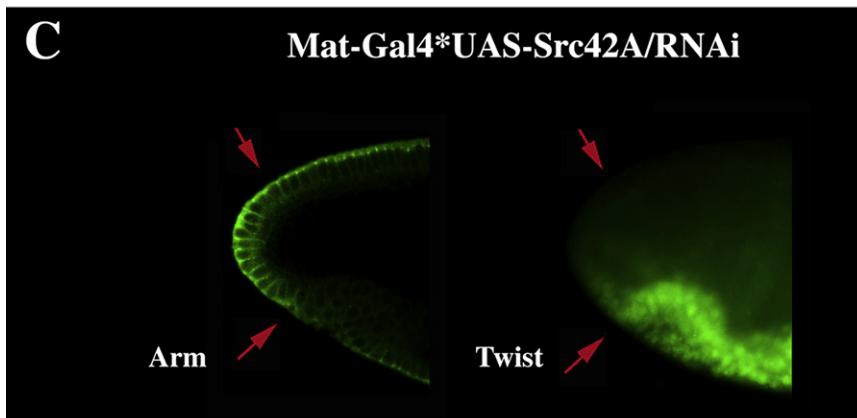
**Figure 3. Mechanical Activation of Arm Nuclear Translocation Depends on Src42A**

(A) Arm protein is shown in green. (B) Nuclear accumulation of Arm, normalized to junctional Arm quantity, is compared across various experimental conditions. Error bars are standard deviations. (C) Effects of Src42A/RNAi on Arm (left), and Twist (right), in the stomodeal cells at stage 7. For (A) and (C), the 15 sagittal stomodeal cells are bracketed by red arrows. Note that in ablated rescued embryos, stomodeal cells moved due to magnetic tweezers manipulation. DAPI was systematically used as a counterstain to check that confocal optical sections fully cross stomodeal cell nuclei (data not shown).

**B**



**C**



nuclear Arm increased  $1.76 \pm 0.33$ -fold during this period. In the stage 9 embryonic ectoderm, comparing Wingless/Wnt-responding cells to their nonresponding neighbors revealed a  $1.67 \pm 0.16$ -fold difference in nuclear Arm accumulation (see Figure S4). Thus, the changes in Arm associated with stomodeal compression are consistent with the idea that mechanical strain triggers transcriptionally active levels of nuclear Arm.

### Src42A Is Required for Mechanical Induction of Arm Nuclear Translocation and Twist Expression

In *Drosophila* embryos, Src42A can trigger cytosolic and nuclear accumulation of Arm (Shindo et al., 2008; Takahashi et al., 2005). In mammalian cells, p-Src has been shown to directly inactivate the site of interaction of its substrate  $\beta$ -catenin with E-cadherin, by Y654 phosphorylation (Piedra et al., 2001). In addition, Src kinases are either mechanically activated (Wang et al., 2005) or permissively necessary (Sawada et al., 2006) key elements of cells' mechano-transduction signaling. We thus considered Src42A as a likely upstream candidate involved in mechanical activation of Arm nuclear translocation. To probe the role of Src42A in Arm nuclear translocation during the compression of the stomodeal cells, we used the UAS-Src42A/RNAi transgenic line. This strain showed no gastrulation defect at early developmental stages. At stage 7, however, the Mat-Gal4\*UAS-Src42A/RNAi progeny behaved as though they did not respond to compression: they retained Arm in their cellular junctions (Figure 3C), while Arm levels in the nucleus ( $\alpha_{N/J} = 1.25 \pm 0.22$ ) and cytoplasm ( $\alpha_{C/J} = 1.49 \pm 0.28$ ) remained low (Figure 3B for  $\alpha_{N/J}$ ). Concomitantly, we found that Src42A/RNAi caused a pronounced defect in Twist expression, characterized by a drop of the  $I_s/I_m$  ratio to  $30\% \pm 12\%$  ( $n = 20$ ), comparable to the  $18\% \pm 10\%$  Twist expression in uncompressed stomodeal cells of ablated embryos (Figure 3C and Figure 2D). Similar results were obtained from a dominant negative form of Src42A for which a K295M mutation was introduced in the catalytic domain (see Supplemental Results and Figure S5A).

In order to determine whether tissue deformation regulates Src activity, we checked the phosphorylation state of Src42A by labeling embryos with a specific antibody against the activated p-Src42A phosphorylated form (Shindo et al., 2008). We found the presence of p-Src42A at stages 5 and 6 in stomodeal cells, before stage 7 compression (Figure S5B). In both the unperturbed and ablated stage 7 embryos, we found similar expression of p-Src42A in stomodeal cells (Figure S5B). In addition, expression of an activated form of Src42A (using Hkb-Gal4\*UAS-Src<sup>act</sup>), in ablated embryos defective in stomodeal cell compression, did not rescue Arm nuclear translocation ( $\alpha_{N/J} = 1.16 \pm 0.31$  and  $\alpha_{C/J} = 1.32 \pm 0.30$ ,  $n = 20$ ) or Twist expression ( $I_s/I_m = 35\% \pm 29\%$ ,  $n = 18$ ) (Figure S5C). Together these results suggest that Src42A is not responsive to tissue deformation in this context, that Src hyperactivation is not sufficient to rescue the effects of mechanical compression, and thus that Src42A acts upstream of Arm in a permissive rather than an instructive manner in stomodeal cells.

### Mechanical Induced Levels of Twist Expression Control Stomodeal Cell Differentiation

Finally, we examined the physiological function of Twist expression in stomodeal cells at stage 7. These cells participate in the

formation of the anterior midgut (aMG) primordium at stage 9 (Technau and Campos-Ortega, 1985). To test whether the high level of Twist expression in stomodeal cells at stage 7 is needed for subsequent aMG formation or differentiation, we knocked down expression of Twist in stomodeal cells at stage 7, using Hkb-Gal4 to drive UAS-Twi/RNAi. Prior to stage 6, the UAS/Gal4 interaction is not efficient using zygotic drivers (Brand et al., 1994); thereafter, the overlapping domain of *hkb* with *twi* expression is restricted to the stomodeal primordium from stage 7 to stage 8, the last stage of Twist expression in the stomodeum (McDonald and Doe, 1997; Thisse et al., 1988) (see Supplemental Experimental Procedures). We found that our approach did attenuate Twist levels ( $I_s/I_m = 33\% \pm 13\%$ ,  $n = 13$ ) in stomodeal cells, beginning at late stage 7 (Figure 4A and Figure 2D). This decrease in Twist expression is quantitatively comparable to the decrease observed in ablated (compression-defective) or Src/Arm signaling-defective embryos (Figure 2D). Since our ferrofluid injection protocol is incompatible with development beyond stage 8 (see Figure S3 and further discussion in Supplemental Results), the Hkb-Gal4\*UAS-Twi/RNAi progeny were used to quantitatively mimic the defect in Twist expression seen in embryos lacking GBE dependent compression.

The expression of the endodermal determinant Dve was analyzed in the Hkb-Gal4\*UAS-Twi/RNAi progeny. Dve is required for copper and interstitial cell fate specification, leading to functional digestive cells in the larva (Fuss and Hoch, 1998; Nakagoshi et al., 1998). In wild-type embryos, Ubx and AbdA expression in the visceral mesoderm parasegments 7 and 8 induces the expression of Dve in the middle midgut (mMG) (Nakagoshi et al., 1998; Thuringer and Bienz, 1993). In stage 14 embryos, Dve is expressed over a belt of  $18 \pm 3$  cells localized in ventral mMG sagittal sections ( $n = 18$ ) (Figure 4B). At stage 15, after mMG endodermal cells have completely surrounded the yolk, MG constrictions appear and the formation of 4 separated lobes initiates, in which lobes 2 and 3 are Dve positive (Nakagoshi et al., 1998; Thuringer and Bienz, 1993). In the sagittal plane, lobe 2 consists of  $24 \pm 6$  Dve-positive cells and lobe 3 of  $17 \pm 5$  Dve-positive cells ( $n = 12$ ) (Figure 4B). We found that the Hkb-Gal4\*UAS-Twi/RNAi progeny exhibit significant defects in anterior mMG differentiation, noticeable at stages 14 and 16. For 72% of the progeny ( $n = 18$ ), the expression domain of Dve at stage 14 is reduced to a belt of only  $6 \pm 1$  cells (Figure 4B). In addition, for 95% of the progeny at stage 16 ( $n = 18$ ), Dve expression was defective in the anterior lobe 2, exhibiting a mean value of  $6.5 \pm 2$  Dve-positive cells. Forty-five percent of this pool showed two or fewer Dve-positive cells in lobe 2 (Figure 4B). Deriving from the posterior midgut (pMG) invagination, lobe 3 is surrounded by a normal number of Dve positive cells ( $20 \pm 9$ ). We observed no modification in the expression of Labial (Hoppler and Bienz, 1994) in the same cells (data not shown), indicating restricted effects on Dve. Finally, 86% of Hkb-Gal4\*UAS-Twi/RNAi larvae died at third instar stage ( $n = 139$ ). Neither the Hkb-Gal4 nor the UAS-Twi/RNAi exhibited any anomalous Dve or lethal phenotype within the same conditions (data not shown). The Hkb-Gal4 driver coupled to the UAS dominant negatives of TCF or of Src42A were not used because of the overlap of the TCF, Wg, and Src42A patterns with Hkb expression pattern that are not specific to stomodeal cells at stage 7 (McDonald and Doe, 1997; Schmidt-Ott and Technau, 1992; Takahashi et al., 2005; van de Wetering et al., 1997).

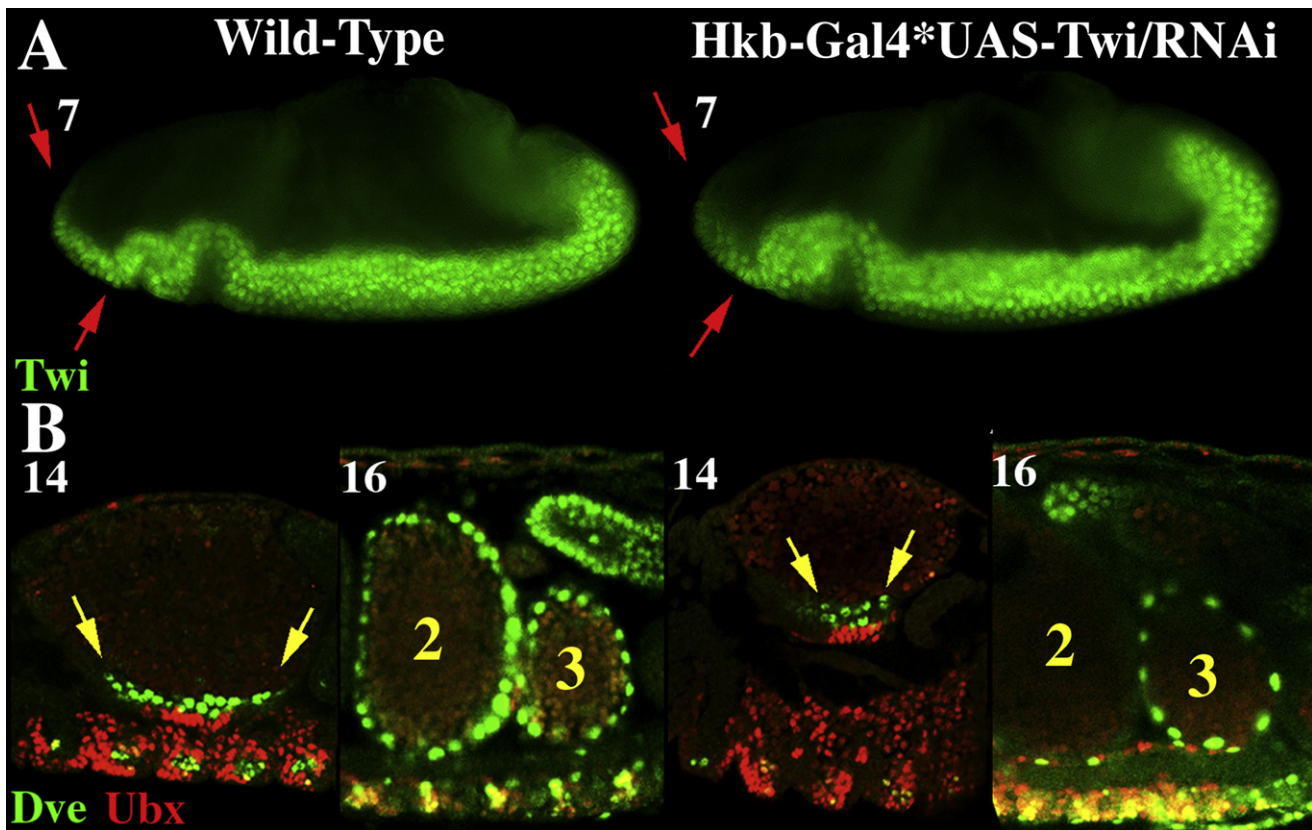


**Figure 4. Quantitative Effect of Twist on Stomodeal Cell Differentiation**

(A) Low Twist expression in late stage 7 Hkb-Gal4\*UAS-Twi/RNAi embryos at 28°C, in which expression of Twist/RNAi is specifically induced in stomodeal cells, compared to wild-type embryos.

(B) Dve labeling of stage 14 and stage 16 middle midgut of Hkb-Gal4\*UAS-Twi/RNAi embryos as compared to the wild-type. Dve is expressed in the endoderm (green, yellow arrows). Ubx is expressed in the visceral mesoderm (red), observed in confocal microscopy.

In stage 7 Hkb-Gal4\*UAS-Twi/RNAi embryos, the silencing of Twist does not occur in the mesoderm from which the visceral mesoderm is derived (Reuter et al., 1993); rather it is specific to the stomodeal cells that participate in the development of the aMG, which fuses with the pMG at stage 13 to form the mMG (Hartenstein et al., 1985), and quantitatively mimics the lack of Twist expression associated with the lack of mechanical signaling in stomodeal cells. Thus, the high level of Twist expression dependent on mechanical induction is required for the proper differentiation of the anterior mMG.

## DISCUSSION

Demonstrating the role of mechanical deformations in the regulation of developmental gene expression requires an ability to reproduce endogenous deformations by locally controlling tissue deformations within the living embryo. Although tools for measuring and applying global forces had been previously reported for studying *Xenopus* embryo tissue explants (Moore, 1994), approaches for locally manipulating tissues within developing embryos were still lacking. Here, magnetized cells were remotely manipulated to produce a  $60 \pm 20$  nN force necessary to generate deformations similar to those produced endogenously. The magnitude of this force is smaller by a factor of

$\sim 20$  than the  $1 \mu\text{N}$  force associated with the convergent extension movements in *Xenopus* explants measured using the deflection of an optical fiber (Moore, 1994). This is consistent with the fact that the *Xenopus* embryo is 10 times larger than the *Drosophila* embryo. This value is also consistent with the 13 nN force developed by a 20 MDCK cell assembly on a soft micropillar surface, noting that the cell colony is five times smaller than the *Drosophila* embryo length (Saez et al., 2007). Importantly, both magnetic and external uncontrolled forces rescued mechano-sensitive Twist expression in the stomodeum. This indicates that Twist expression might not be highly sensitive to the intensity or symmetry of tissue deformations.

The remote manipulation of magnetized cells in the *Drosophila* embryo enabled us to demonstrate that mechanical compression of stomodeal cells comparable to those induced by endogenous morphogenetic movements upregulates Twist expression in the stomodeal primordium. We also show that Arm nuclear translocation is a major instructive step in the mechanical-to-genetic transduction pathway, coupling the macroscopic events of morphogenetic shape changes to the molecular processes regulating developmental gene expression. Moreover, previous studies showed that Src family kinases are involved in mechano-transduction through two distinct modes: either through direct mechanical activation resulting in phosphorylation of Src

(Wang et al., 2005), or through a permissive mode where a mechanically induced conformational change in a Src substrate makes its phosphorylation site accessible to the already activated p-Src (Sawada et al., 2006). Here we find that Src42A acts in the permissive mode in the mechano-transduction pathway upstream of Arm. Because  $\beta$ -catenin is a substrate of Src in mammalian cells (Piedra et al., 2001), one might speculate that the mechano-sensitive substrate of p-Src42A in *Drosophila* embryos may be junctional Arm. Further study will be necessary to determine whether this is the case, or if an unknown mechano-sensitive Src42A substrate controls Arm activation.

At later stages of development during organogenesis, mechanical cues generated by organ functions were also suggested to shape the physiological function of specialized organs (le Noble et al., 2004). For instance, embryonic muscle activity is involved in mouse bone development through  $\beta$ -catenin activation (Hens et al., 2005). Here we find that endogenous morphogenetic movements at early stages of development are able to control gene expression, which identifies a feedback loop of the embryo morphological development onto the genome. Such mechanical cues may mediate long-range effects that coordinate and synchronize differentiation events throughout the whole embryo. Such effects may be especially important under conditions in which dynamical and complex topology prevents the establishment of the long-range morphogen gradients that are efficient at earlier stages, when cells are arranged in simpler, static geometrical patterns.

## EXPERIMENTAL PROCEDURES

### Deformation Techniques

Tissue ablations were carried out using a custom-built multiphoton microscope by performing slow line scans of the focused laser beam (820 nm, 130 fs, 76 MHz) across dorsal cells as described previously (Supatto et al., 2005). Two-photon imaging was performed on the same setup. After the photoablation procedure, ferrofluid (gift of V. Cabuil) injections were performed following standard injection protocols (Wilkie and Davis, 2001) with a Femto-Jet (Eppendorf, France). Thirty picoliters of a  $5 \text{ mol l}^{-1}$  solution of  $\gamma\text{Fe}_2\text{O}_3$  nanosized magnetic core coated with citrates (Mayer et al., 1999) were injected at the end of cellularization into the yolk, near the basal surface of the antero-dorsal cells adjacent to the stomodeum. Injected ferrofluid was subsequently attracted into the cells (still basally opened at this stage) by using an electromagnetic tip, brought to  $10 \mu\text{m}$  from the target cells. Once the electromagnet was removed, magnetized antero-dorsal cells were dragged toward the anterior pole at mid-stage 6 by a magnetic field gradient parallel to the antero-posterior axis of the embryo, supplied by magnetic tweezers consisting of two cylindrical permanent magnets mounted in an antiparallel configuration (see Supplemental Experimental Procedures for details and evaluation of the force).

### Deformation Analysis

Deformation analysis was performed using image correlation techniques adapted from particle image velocimetry (PIV) (Supatto et al., 2005). We estimated the velocity fields in the sagittal plane from two-photon image sequences of sGMCA lines using algorithms based on MatPIV with coarse graining (a PIV software package written by Johan Kristian Sveen for use with MATLAB), and deduced strain rate patterns by calculating the mean value of the velocity field divergence over 3 min. The divergence is the difference of velocity between neighbor cells and leads to the deformation field (if neighbor cells progress with the same velocity, there is no deformation). All experiments were carried at  $19 \pm 1^\circ\text{C}$ .

### Genetics and Labeling

Immunochemistry was performed according to standard protocols (Lehmann and Tautz, 1994). Secondary antibodies were anti-rabbit Alexa488 and Alexa594 (Molecular Probes, Eugene, OR), and anti-mouse Cy3 (Jackson

ImmunoResearch, USA). Any labeling of genetically or mechanically perturbed embryos was made in parallel with Oregon R controls, using the same tube of antibodies, in triplicate independent experiments. UAS<sup>+</sup>Gal4 crosses were performed at  $28^\circ\text{C}$ , except for the larvae viability test, which appeared to be efficient after  $30^\circ\text{C}$  crosses. Epifluorescence microscopy observations were done under a Leica (Leica Microsystems, France) DMIRB microscope with a CA-742 95 Hamamatsu (Hamamatsu Photonics, France) camera. Confocal microscopy was performed on a Leica SP2 microscope. Fly strains used are described in the Supplemental Experimental Procedures.

### Fluorescence Measurements

The ratio of stomodeal-to-mesodermal Twist expression ( $I_{\text{S}}/I_{\text{M}}$ ) was estimated from fluorescent images of Twist immuno-labeling. The mean value of fluorescence intensity per pixel was measured in nine representative nuclei from the anterior (three nuclei), middle (three nuclei), and posterior (three nuclei) domains of the stomodeum, and the background signal in the surrounding yolk was subtracted. This was normalized to the maximal fluorescence intensity of the mesoderm, measured following the same procedure.

Similar analyses were carried out to quantify Armadillo localization in the cytoplasm and the nucleus of stomodeal cells following:

$$\alpha_{N/J} = \frac{[Arm]_N/[Arm]_J \parallel_{after}}{[Arm]_N/[Arm]_J \parallel_{before}}$$

The maximum of the intensity profile passing through cell junctions assessed Armadillo concentration at the level of cell junctions. Image J software was used to analyze images. All data presented a statistically high significance compared to associated controls, as systematically checked by a  $p < 0.001$  by Student's t test.

## SUPPLEMENTAL DATA

Supplemental Data include five figures, two movies, Supplemental Experimental Procedures, Supplemental Results, and Supplemental References and can be found with this article online at <http://www.developmentalcell.com/cgi/content/full/15/3/470/DC1/>.

## ACKNOWLEDGMENTS

We thank Padra Ahmadi, Emilie Henry, Catherine Schaffner, and Nicolas Olivier for technical help, Rolf Reuter, Ryu Ueda, Siegfried Roth, Bernhard Fuss, Rob White, Ruth Montague, Vincent Croquette, and Valérie Cabuil for sending biological and magnetic materials, Jean-Claude Bacri and Eric Brouzés for discussions on magnetic experiments, Shigeo Hayashi for discussions on Src42A, J.K. Sveen for providing MatPIV, and Joanne Whitehead and Steve Cohen for comments on the manuscript. This research was supported by the INSERM and the CNRS, the Association pour la Recherche contre le Cancer, the Institut Curie, by the Human Science Frontiers Program, and in part by the Ecole Centrale Paris and by Microsoft Research through the European Program. N.D. performed the magnetic experiment and W.S. the microneedle manipulation. P.A.P. performed the PIV analysis. E.B. designed the optical experiments and participated in the magnetic experiments. E.F. designed the magnetic and microneedle experiments, and coordinated the study.

Received: November 15, 2007

Revised: May 16, 2008

Accepted: July 23, 2008

Published: September 15, 2008

## REFERENCES

- Brand, A.H., Manoukian, A.S., and Perrimon, N. (1994). Ectopic expression in *Drosophila*. *Methods Cell Biol.* 44, 635–654.
- Chen, C.S., Tan, J., and Tien, J. (2004). Mechanotransduction at cell-matrix and cell-cell contacts. *Annu. Rev. Biomed. Eng.* 6, 275–302.
- Costa, M., Sweeton, D., and Wieschaus, E. (1993). Gastrulation in *Drosophila*: cellular mechanisms of morphogenetic movements. In *The Development of*

- Drosophila melanogaster*, M. Bate and A. Martinez-Arias, eds. (Cold Spring Harbor, NY: Cold Spring Harbor Laboratory Press), pp. 425–464.
- Farge, E. (2003). Mechanical induction of twist in the *Drosophila* foregut/stomodaeal primordium. *Curr. Biol.* **13**, 1365–1377.
- Fuss, B., and Hoch, M. (1998). *Drosophila* endoderm development requires a novel homeobox gene which is a target of Wingless and Dpp signalling. *Mech. Dev.* **79**, 83–97.
- Hartenstein, V., Technau, G.M., and Campos-Ortega, J.A. (1985). Fate-mapping in wild-type *Drosophila melanogaster*. *Roux Arch. Dev. Biol.* **194**, 213–216.
- Heasman, J., Crawford, A., Goldstone, K., Garner-Hamrick, P., Gumbiner, B., McCrean, P., Kintner, C., Noro, C.Y., and Wylie, C. (1994). Overexpression of cadherins and underexpression of  $\beta$ -catenin inhibit dorsal mesoderm induction in early *Xenopus* embryos. *Cell* **79**, 791–803.
- Hens, J.R., Wilson, K.M., Dann, P., Chen, X., Horowitz, M.C., and Wysolmerski, J.J. (2005). TOPGAL mice show that the canonical Wnt signaling pathway is active during bone development and growth and is activated by mechanical loading in vitro. *J. Bone Miner. Res.* **20**, 1103–1113.
- Hoppler, S., and Bienz, M. (1994). Specification of a single cell type by a *Drosophila* homeotic gene. *Cell* **76**, 689–702.
- Hufnagel, L., Teleman, A.A., Rouault, H., Cohen, S.M., and Shraiman, B.I. (2007). On the mechanism of wing size determination in fly development. *Proc. Natl. Acad. Sci. USA* **104**, 3835–3840.
- Irvine, K.D., and Wieschaus, E. (1994). Cell intercalation during *Drosophila* germband extension and its regulation by pair-rule segmentation genes. *Development* **120**, 827–841.
- Keller, R. (2002). Shaping the vertebrate body plan by polarized embryonic cell movements. *Science* **298**, 1950–1954.
- le Noble, F., Moyon, D., Pardanaud, L., Yuan, L., Djonov, V., Matthijsen, R., Breant, C., Fleury, V., and Eichmann, A. (2004). Flow regulates arterial-venous differentiation in the chick embryo yolk sac. *Development* **131**, 361–375.
- Lehmann, R., and Tautz, D. (1994). In situ hybridation to RNA. In *Drosophila melanogaster: Practical Uses in Cell and Molecular Biology*, L.S.B. Glodstein and E.A. Fyrberg, eds. (San Diego: Academic Press), pp. 575–598.
- Matthews, B.D., Overby, D.R., Mannix, R., and Ingber, D.E. (2006). Cellular adaptation to mechanical stress: role of integrins, Rho, cytoskeletal tension and mechanosensitive ion channels. *J. Cell Sci.* **119**, 508–518.
- Mayer, C.R., Cabuil, V.V., Lalot, T., and Thouvenot, R. (1999). Incorporation of magnetic nanoparticles in new hybrid networks based on heteropolyanions and polyacrylamide. *Angew. Chem. Int. Ed. Engl.* **38**, 3672–3675.
- McDonald, J.A., and Doe, C.Q. (1997). Establishing neuroblast-specific gene expression in the *Drosophila* CNS: huckebein is activated by Wingless and Hedgehog and repressed by Engrailed and Gooseberry. *Development* **124**, 1079–1087.
- Moore, S.W. (1994). A fiber optic system for measuring dynamic mechanical properties of embryonic tissues. *IEEE Trans. Biomed. Eng.* **41**, 45–50.
- Nakagoshi, H., Hoshi, M., Nabeshima, Y., and Matsuzaki, F. (1998). A novel homeobox gene mediates the Dpp signal to establish functional specificity within target cells. *Genes Dev.* **12**, 2724–2734.
- Nelson, W.J., and Nusse, R. (2004). Convergence of Wnt,  $\beta$ -catenin, and cadherin pathways. *Science* **303**, 1483–1487.
- Norvell, S.M., Alvarez, M., Bidwell, J.P., and Pavalko, F.M. (2004). Fluid shear stress induces  $\beta$ -catenin signaling in osteoblasts. *Calcif. Tissue Int.* **75**, 396–404.
- Peifer, M., and Wieschaus, E. (1990). The segment polarity gene armadillo encodes a functionally modular protein that is the *Drosophila* homolog of human plakoglobin. *Cell* **63**, 1167–1176.
- Piedra, J., Martinez, D., Castano, J., Miravet, S., Dunach, M., and de Herreros, A.G. (2001). Regulation of beta-catenin structure and activity by tyrosine phosphorylation. *J. Biol. Chem.* **276**, 20436–20443.
- Reuter, R., Grunewald, B., and Leptin, M. (1993). A role for the mesoderm in endodermal migration and morphogenesis in *Drosophila*. *Development* **119**, 1135–1145.
- Saez, A., Ghibaudo, M., and Buguin, A. (2007). Rigidity-driven growth and migration of epithelial cells on microstructured anisotropic substrates. *Proc. Natl. Acad. Sci. USA* **104**, 8281–8286.
- Sanson, B., White, P., and Vincent, J.P. (1996). Uncoupling cadherin-based adhesion from wingless signalling in *Drosophila*. *Nature* **383**, 627–630.
- Sawada, Y., Tamada, M., Dubin-Thaler, B.J., Cherniavskaya, O., Sakai, R., Tanaka, S., and Sheetz, M.P. (2006). Force sensing by mechanical extension of the Src family kinase substrate p130Cas. *Cell* **127**, 1015–1026.
- Schmidt-Ott, U., and Technau, G.M. (1992). Expression of en and wg in the embryonic head and brain of *Drosophila* indicates a refolded band of seven segment remnants. *Development* **116**, 111–125.
- Shindo, M., Wada, H., Kaido, M., Tateno, M., Aigaki, T., Tsuda, L., and Hayaishi, S. (2008). Dual function of Src in the maintenance of adherens junctions during tracheal epithelial morphogenesis. *Development* **135**, 1355–1364.
- Solnica-Krezel, L. (2005). Conserved patterns of cell movements during vertebrate gastrulation. *Curr. Biol.* **15**, R213–R228.
- Somogyi, K., and Rorth, P. (2004). Evidence for tension-based regulation of *Drosophila* MAL and SRF during invasive cell migration. *Dev. Cell* **7**, 85–93.
- Supatto, W., Débarre, D., Moulia, B., Brouzés, E., Martin, J.-L., Farge, E., and Beaurepaire, E. (2005). *In vivo* modulation of morphogenetic movements in *Drosophila* embryos with femtosecond laser pulses. *Proc. Natl. Acad. Sci. USA* **102**, 1047–1052.
- Takahashi, M., Takahashi, F., Ui-Tei, K., Kojima, T., and Saigo, K. (2005). Requirements of genetic interactions between Src42A, armadillo and shotgun, a gene encoding E-cadherin, for normal development in *Drosophila*. *Development* **132**, 2547–2559.
- Technau, G.M., and Campos-Ortega, J.A. (1985). Fate mapping in wild-type *Drosophila melanogaster*. II- Injections of horseradish peroxidase in cells of the early gastrula stage. *Roux Arch. Dev. Biol.* **194**, 196–212.
- Thisse, B., Stoetzel, C., Gorostiza-Thisse, C., and Perrin-Schmitt, F. (1988). Sequence of the twist gene and nuclear localization of its protein in endomesodermal cells of early *Drosophila* embryos. *EMBO J.* **7**, 2175–2183.
- Thüringer, F., and Bienz, M. (1993). Indirect autoregulation of a homeotic *Drosophila* gene mediated by extracellular signaling. *Proc. Natl. Acad. Sci. USA* **90**, 3899–3903.
- van de Wetering, M., Cavallo, R., Dooijes, D., van Beest, M., van Es, J., Louriéro, J., Ypma, A., Hursh, D., Jones, T., Bejsovec, A., et al. (1997). Armadillo coactivates transcription driven by the product of the *Drosophila* segment polarity gene dTCF. *Cell* **88**, 789–799.
- Wang, Y., Botvinick, E.L., Zhao, Y., Berns, M.W., Usami, S., Tsien, R.Y., and Chien, S. (2005). Visualizing the mechanical activation of Src. *Nature* **434**, 1040–1045.
- Wilkie, G.S., and Davis, I. (2001). *Drosophila* wingless and pair-rule transcripts localize apically by dynein-mediated transport of RNA particles. *Cell* **105**, 209–219.